JACC: BASIC TO TRANSLATIONAL SCIENCE
VOL. 2, NO. 6, 2017
ISSN 2452-302X
https://doi.org/10.1016/j.jacbts.2017.06.007

PRECLINICAL RESEARCH

Protein Kinase C Inhibition With Ruboxistaurin Increases Contractility and Reduces Heart Size in a Swine Model of Heart Failure With Reduced Ejection Fraction

Thomas E. Sharp III, BA,[a] Hajime Kubo, PhD,[a] Remus M. Berretta, BS,[a] Timothy Starosta, BS,[b] Markus Wallner, MD, PhD,[a] Giana J. Schena, BS,[a] Alexander R. Hobby, BS,[a] Daohai Yu, PhD,[c] Danielle M. Trappanese, PhD,[a] Jon C. George, MD,[a,d] Jeffery D. Molkentin, PhD,[e] Steven R. Houser, PhD[a]

VISUAL ABSTRACT

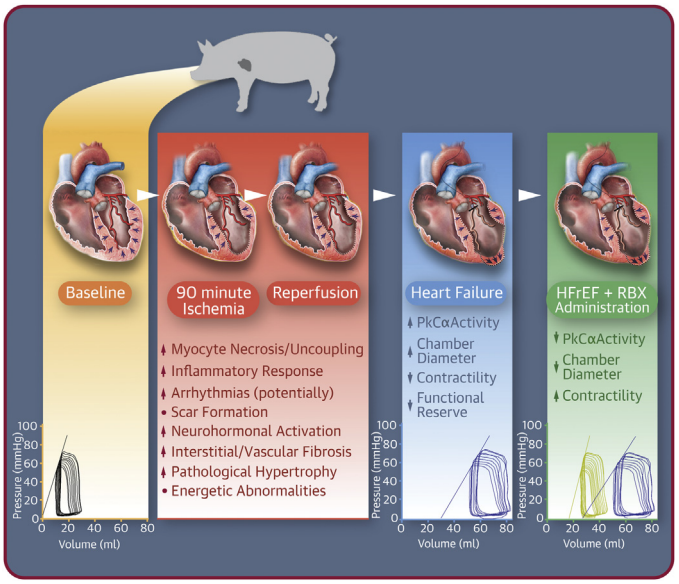

Sharp, T.E. et al. J Am Coll Cardiol Basic Trans Science. 2017;2(6):669-83.

HIGHLIGHTS

- **Acute protein kinase A α (PKCα) inhibition with ruboxistaurin reduces heart size post-myocardial infarction.**
- **Acute PKCα inhibition with ruboxistaurin increases contractility post-myocardial infarction.**
- **PKCα phosphorylation at Thr638 is positively correlated to increases in left ventricular volumes and reduced ejection fraction, indicative of disease progression.**

From the [a]Cardiovascular Research Center, Department of Physiology, Temple University Lewis Katz School of Medicine, Philadelphia, Pennsylvania; [b]Department Cardiology, Johns Hopkins University School of Medicine, Baltimore, Maryland; [c]Department of Clinical Sciences, Temple Clinical Research Institute, Temple University Lewis Katz School of Medicine, Philadelphia, Pennsylvania; [d]Department of Cardiology, Temple University Hospital, Philadelphia, Pennsylvania; and the [e]Department of Pediatrics and Howard Hughes Medical Institute, Cincinnati Children's Hospital Medical Center, Cincinnati, Ohio. This work was supported by the National Institutes of Health, NHLBI - Project Program Grant (5P01HL108806-04) (to Drs. Molkentin and Houser). Mr. Sharp received pre-doctoral fellowship funding from the American Heart Association (14PRE20450006). Eli Lilly & Company provided the drug (ruboxistaurin) to Dr. Molkentin for this current study. The authors have reported that they have no relationships relevant to the contents of this paper to disclose.

All authors attest they are in compliance with human studies committees and animal welfare regulations of the authors' institutions and Food and Drug Administration guidelines, including patient consent where appropriate. For more information, visit the *JACC: Basic to Translational Science* author instructions page.

Manuscript received March 16, 2017; revised manuscript received May 10, 2017, accepted June 20, 2017.

JACC: BASIC TO TRANSLATIONAL SCIENCE VOL. 2, NO. 6, 2017
DECEMBER 2017:669–83

ABBREVIATIONS AND ACRONYMS

ADHF = acute decompensated heart failure

DIG = digitalis

DOB = dobutamine

ECG = electrocardiogram

EDPVR = end-diastolic pressure-volume relationship

EDV = end-diastolic volume

E_{es} = elastance end-systole

ESPVR = end-systolic pressure-volume relationship

ESV = end-systolic volume

HF = heart failure

HFrEF = heart failure with reduced ejection fraction

IR = ischemia-reperfusion

LAD = left anterior descending coronary artery

LV = left ventricle/ventricular

LVEDV = left ventricular end-diastolic volume

LVEF = left ventricular ejection fraction

$LVVP_{ed}10$ = left ventricular end-diastolic volume at a pressure of 10 mm Hg

$LVVP_{es}80$ = left ventricular end- systolic volume at a pressure of 80 mm Hg

MI = myocardial infarction

PKA = protein kinase A

PKC = protein kinase C

PLN = phospholamban

PRSW = pre-load recruitable stroke work

RBX = ruboxistaurin

SUMMARY

Inotropic support is often required to stabilize the hemodynamics of patients with acute decompensated heart failure; while efficacious, it has a history of leading to lethal arrhythmias and/or exacerbating contractile and energetic insufficiencies. Novel therapeutics that can improve contractility independent of beta-adrenergic and protein kinase A-regulated signaling, should be therapeutically beneficial. This study demonstrates that acute protein kinase C-α/β inhibition, with ruboxistaurin at 3 months' post-myocardial infarction, significantly increases contractility and reduces the end-diastolic/end-systolic volumes, documenting beneficial remodeling. These data suggest that ruboxistaurin represents a potential novel therapeutic for heart failure patients, as a moderate inotrope or therapeutic, which leads to beneficial ventricular remodeling. (J Am Coll Cardiol Basic Trans Science 2017;2:669–83)

Cardiac pump function is reduced in heart failure (HF) secondary to acute myocardial infarction (MI) and other diseases that cause ventricular dilation. In addition to reductions in basal function, there is a lack in contractile reserve (1). This syndrome is termed HF with reduced ejection fraction (HFrEF). Inotropic therapy is often required to improve pump function and support central hemodynamics in acute decompensated HF (ADHF) (2). However, most inotropic agents currently in clinical practice activate protein kinase A (PKA) or alter key downstream inotropic mediators (3). PKA signaling is the principle mechanism to regulate cardiac contractility in the normal heart. Persistent activation of PKA signaling is required in the failing heart to maintain central hemodynamics, and this leads to disruption of the signaling cascade and blunted adrenergic responsiveness. Drugs such as milrinone increase cyclic adenylate monophosphate (cAMP) by inhibiting the phosphodiesterase (PDE III in this case) that catalyze cAMP inactivation and thereby increase PKA activation. These drugs have reduced efficacy when compared with the normal heart, but are still potent inotropes that can improve cardiac function in patients who present with ADHF (4). However, these drugs can induce lethal arrhythmias (5), and because they can also cause Ca^{2+} overload in the sarcoplasmic reticulum (SR), they can induce myocyte death (6) and thereby exacerbate HF progression. Therefore, patients that survive episodes of ADHF that required the use of PKA-activating inotropic support, have a worse prognosis (7). Novel inotropic therapies that increase cardiac contractility and have positive effects on ventricular remodeling, but avoiding PKA signaling, could help patients with HF.

SEE PAGE 684

Over the last decade, we (8–12) and others (13–17) have investigated the role of protein kinase C (PKC) in the alterations of basal inotropy and inotropic reserve in small-animal HF models. PKC is a family of serine/threonine protein kinases, which are activated through Ca^{2+}- and/or lipid-mediated signaling mechanisms, and are enhanced in HF. The major PKC isoform expressed in cardiac tissue of small (mouse) (18) and large (rabbit) (19) animals, as well as in humans, is PKCα (12). PKCα abundance and activity increases in the diseased heart and has been linked to reduced cardiac myocyte contractility, whereas PKCα inhibition increases cardiac contractility (10). PKCα-target proteins are distinct from those activated by PKA (4,20) and include classical Ca^{2+} handling and regulator proteins within the membrane, cytosol, and at the level of sarcomeric proteins (10,15–17,21). Studies performed largely in mouse models suggest that inhibition of PKCα could be a PKA-independent approach to increase contractility in the failing human heart (9,10). However, regulation of cardiac contractility is fundamentally different in rodents and large mammals, including humans, and this may explain why so many Ca^{2+}-dependent therapeutic strategies that have worked in rodent models have not translated to effective therapeutics in humans (22,23). Previously we tested the chronic administration of ruboxistaurin (RBX) in a farm pig model of MI (24). Ladage et al. (24) reported that RBX had beneficial effects on cardiac contractility (dP/dTmax) and remodeling (left ventricular [LV] ejection fraction [LVEF]) at 3 months' post-MI. Although RBX was administered throughout the study (10 mg/kg/day), beneficial effects were only observed at the 3-month time point. This could be due to the normal hypertrophic growth observed in farm pigs over the study timeline or that sufficient cardiac pathology

developed at 3 months post-MI permitting observation of RBX's beneficial effects. This study did not define the mechanism by which RBX treatment improved function, but demonstrated the safety and efficacy of long-term RBX administration post-MI. Therefore, the present study examined the idea that acute PKCα inhibition will increase cardiac contractility in a minipig MI model that has developed significant structural and pathophysiology characteristics consistent with the clinically defined syndrome HFrEF.

The present study explored the effects of a PKCα/β inhibitor, RBX, that has positive inotropic effects in small-animal models of cardiac disease (10,11). RBX is a PKCα/β inhibitor of the bisindolylmaleimide class. It has been tested in clinical trials for patients with diabetic retinopathy (25–27). In these trials, RBX was well tolerated without major side effects, making it an attractive pharmacological agent that could be repurposed for the treatment of patients with HF. The experiments in this study show that acute RBX treatment increased cardiac contractility and reduced heart size (filling volumes) in a swine MI model with ventricular dilation and reduced ejection fraction. These results support the idea that RBX could be a PKA-independent inotropic treatment for patients with HF.

METHODS

STUDY APPROVAL. All animal procedures were approved by Temple University Institutional Animal Care and Use Committee.

ANIMALS, ANESTHESIA INDUCTION, AND MAINTENANCE. Twenty-six female Göttingen minipigs were used (Marshall BioResources, North Rose, New York). All animals were 7 to 8 months of age, with a mean weight of 30 kg. Three groups were derived from this cohort of animals: Sham (n = 6) for gross morphometry, MI + RBX (n = 17), and Control + RBX (n = 3) (**Figure 1**). Anesthesia was induced by intramuscular injection of 6.0 mg/kg tiletamine/zolazepam (Telazol, Fort Dodge Animal Health, Fort Dodge, Iowa). Göttingen minipigs were intubated with an endotracheal tube of 5.5-mm internal diameter, and general anesthesia was maintained with 1% to 2% isoflurane (IsoFlo, Abbott Laboratories, Animal Health Division, Abbott Park, Illinois) supplemented with 100% oxygen. Blood oxygenation was monitored using continuous pulse oximetry. The electrocardiogram (ECG) was monitored throughout the entire procedure.

ISCHEMIA-REPERFUSION INDUCED MI. Induction of ischemia-reperfusion (IR) MI was performed, with slight modification, following previously published methods (28). Briefly, sheaths were introduced into the femoral artery and vein (8-F and 11-F, respectively). Animals were anticoagulated with heparin throughout the procedure using a loading dose of 100 U/kg and a maintenance dose of 40 U/kg every hour. The left anterior descending coronary artery (LAD) was accessed via the right femoral artery using a 6-F 3DRC guide catheter (Cordis, Johnson & Johnson, Miami Lakes, Florida). All animals were administered amiodarone (1.0 mg/kg, intravenous) before MI induction. The 2.5 to 3.0 × 12-mm Maverick angioplasty balloon (Boston Scientific, Natick, Massachusetts) was then inflated to 8.0 atm for a period of 90 min. Next, the balloon was deflated and the guide catheter removed to allow 30 min of reperfusion before sheath removal, which permitted time for any advanced medical intervention that was necessary to treat acute arrhythmias. All animals in the Sham group received the same treatment without inflation of the angioplasty balloon in the LAD. Balloon occlusion and flow restoration were confirmed with angiography (Supplemental Figure 1).

TRANSTHORACIC ECHOCARDIOGRAPHY. Transthoracic echocardiography was performed at baseline, 1 month, 2 months, and 3 months post-MI ± RBX with the Zonare z.one Ultra ultrasound system (Zonare Medical Systems, Mountain View, California). Images were acquired in the 2-dimensional-mode long and short axes; whereas M-mode images were taken in the short axis. All analysis was performed in a blinded manner. End-diastolic dimensions (not shown), end-systolic dimensions (not shown), end-diastolic volume (EDV), end-systolic volume (ESV), and LVEF were calculated following the American Society of Echocardiography guidelines (29).

INVASIVE HEMODYNAMICS. Detailed methods on acquisition/analysis and graphing data have been previously described (30) and can be found in the Supplemental Appendix. Invasive hemodynamics were performed to assess intrinsic cardiac function during systole (i.e., pressure end-systole [P_{es}], volume [V_{es}], LV maximum rate of pressure development [dP/dT], LV $VP_{es}100$, elastance [E_{es}] and volume intercept [V_0]), and diastole (i.e., P_{ed}, V_{ed}, LV minimum dP/dT, LV isovolumic relaxation constant [τ], LV $VP_{ed}10$ and end-diastolic pressure-volume relationship [EDPVR]) at different time points (pre-MI and 3 months post-MI) and under various condition (± dobutamine [DOB, 2.5 μg/kg/min] and/or ± RBX) ([+] = in the presences of substance, [−] = in the absence of substance). Data were plotted with the mean (E_{es}/V_0 [end-systolic pressure-volume

FIGURE 1 Study Timeline

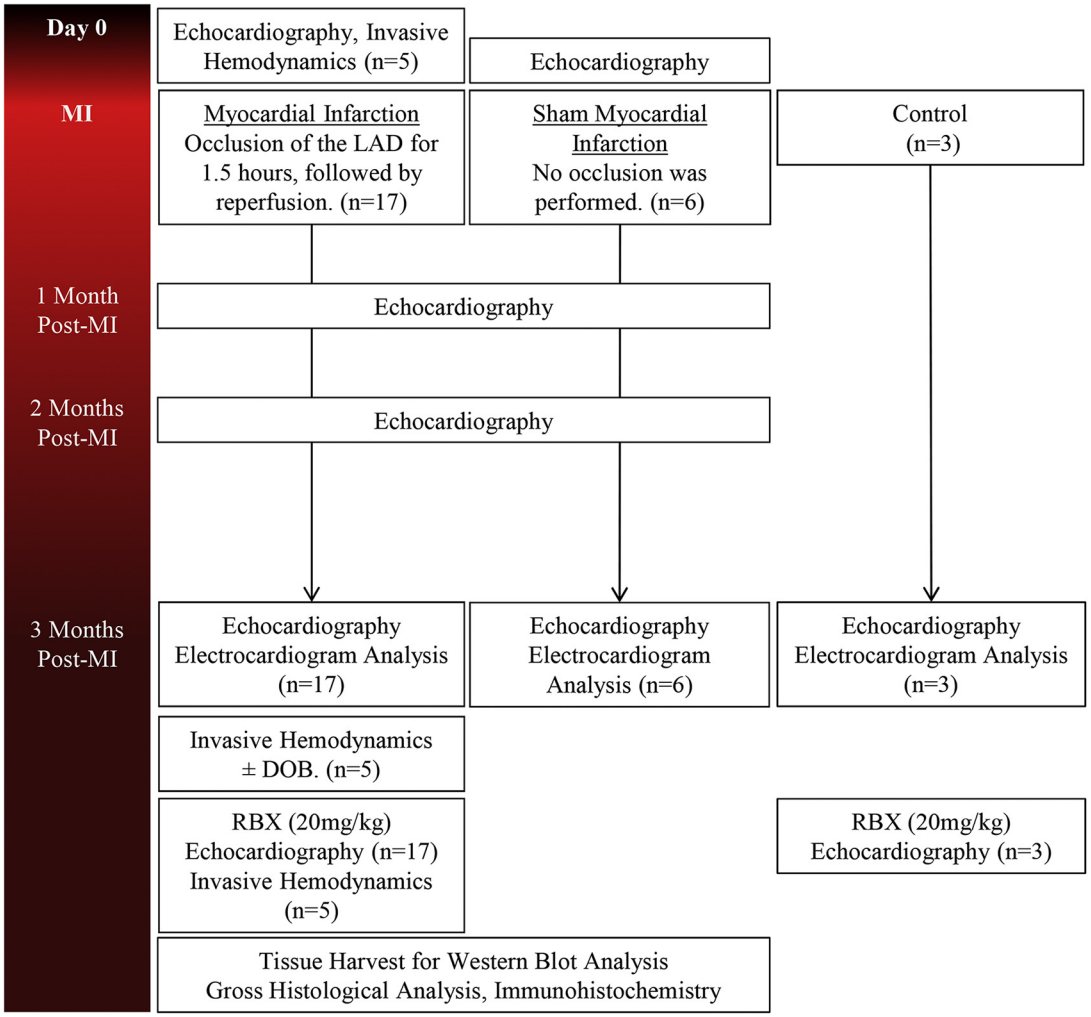

Protocol used to induce acute myocardial infarction (MI) and functionally assess the progression of pathological remodeling. Timeline for delivery of dobutamine (DOB) and ruboxistaurin (RBX) at 3 months' post-MI. LAD = left anterior descending coronary artery.

relationship (ESPVR)] or α/β [EDPVR]) ± SEM to a given set of pressures to observe curve shifts in the ESPVR and EDPVR.

RBX TREATMENT. At 3-month post-MI, a single oral dose of RBX (20 mg/kg) (Eli Lilly and Company, Indianapolis, Indiana) (27) was administered to each animal mixed with normal feed. Animals were given 2 h (31) after RBX administration before any procedure to evaluate function or fulfill any other endpoints (**Figure 1**).

TISSUE PROCESSING AND GROSS MORPHOMETRIC ANALYSIS. Cardiectomy was performed under general anesthesia, and gross morphometry was performed as previously described (28). Briefly, the heart was weighed and the basal two-thirds fixed via perfusion with 2 l of 10% formalin. The bottom one-third was taken for molecular analysis. Further details fully describing tissue processing can be found in the Supplemental Appendix.

PROTEIN ISOLATION, FRACTIONATION, AND WESTERN BLOT ANALYSIS. Frozen tissue samples were taken from the remote zone of the MI animals and a comparable location on sham animals. Protein isolation and fractionation was performed to investigate activation (localization) of PKCα. A subcellular protein fractionation kit was used to separate membrane-bound and cytoplasmic proteins (Thermo Scientific Cat#: 87790, Thermo Fisher Scientific, Waltham,

FIGURE 2 Gross, Cellular, and Molecular Remodeling 3 Months PMI

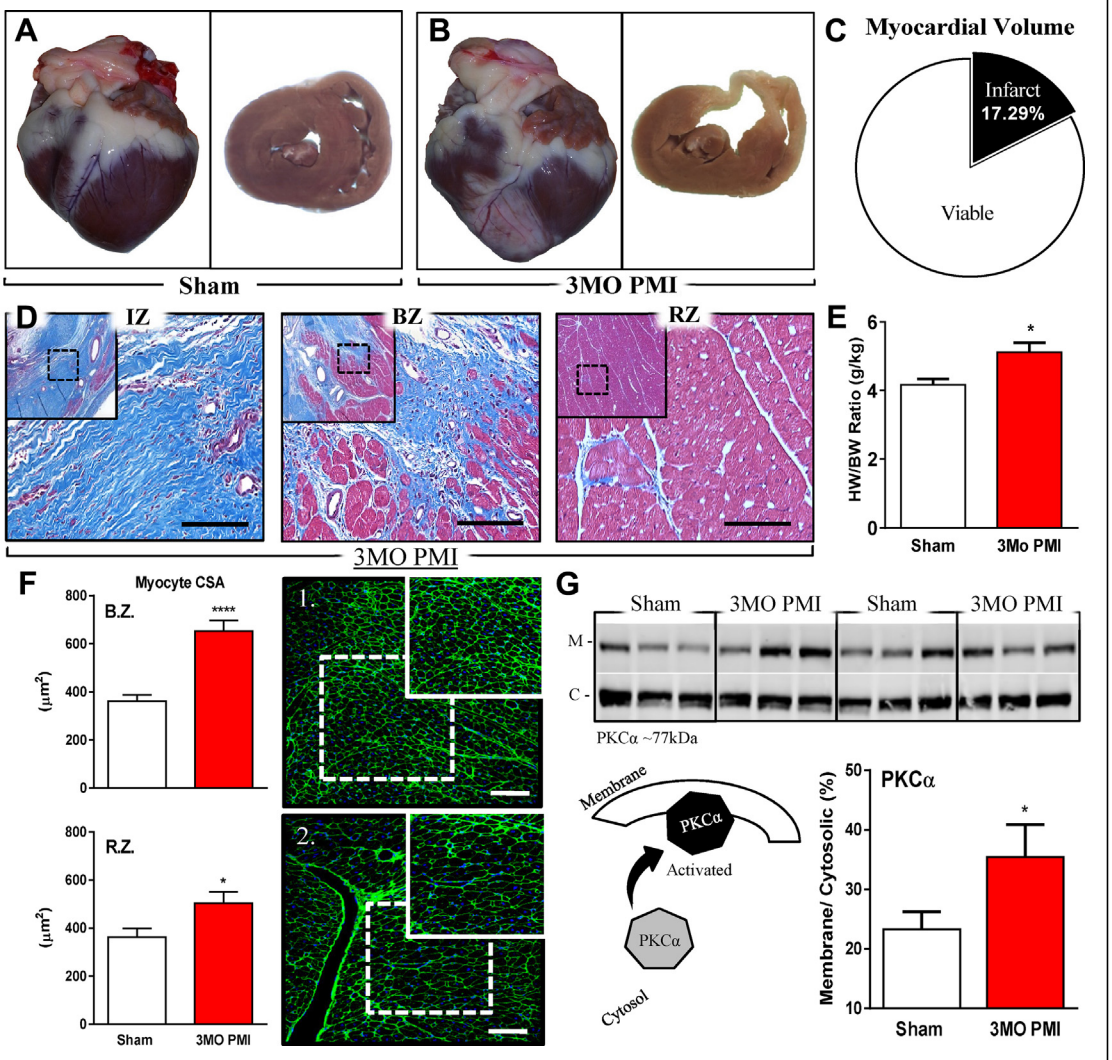

(A) Gross images of sham heart, whole organ **(left)**, and cross section **(right)** of mid-myocardium. **(B)** Gross images of 12-week PMI heart, whole organ **(left)**, and cross section of mid-myocardium **(right)**. **(C)** Scar size analysis showing viable **(white)** and scar tissue **(black)** as a percentage of total myocardial volume at 12 weeks PMI. **(D)** Bright-field images were taken of Masson's trichrome–stained mid-myocardial cross sections of the infarct zone (IZ), border zone (BZ), and remote zone (RZ) of a 3 months PMI animal. The 10× (outside images) and 40× (interior images) were acquired to demonstrate fibrosis and the deposition of collagen in the AW and LW of the PMI animal. **(E)** Heart weight-to-body weight (HW/BW) ratio. **(F)** Myocyte cross-sectional area calculated from the 2 viable zones (border zone [BZ] and remote zone [RZ]) in sham animals versus 3 months PMI animals. The images represent the BZ in the sham group **(F1)** and the 3 months PMI group **(F2)**. Large image is 20× and small image **(top right corner)** is 40×. Data are shown as the mean by anatomic region in the graphs below. **(G)** Animals underwent sham (n = 6) or MI (n = 6) procedure, and terminal studies were performed at 3 months ± PMI. Tissue was collected for molecular analysis. Protein was isolated and fractionated into cytosolic (C) and membrane (M) fractions. Percentage of membrane-bound fraction over the cytosolic fraction is shown. *p ≤ 0.05; ***p ≤ 0.005 versus sham. Large scale bar = 100 μm. Small scale bar = 50 μm. 3 months PMI = 3-month's post-myocardial infarction; other abbreviations as in Figure 1.

Massachusetts) from 200 mg of tissue. Western blots were performed using the LICOR Systems general protocol. Samples were run on a 12% SDS-page gel and transferred overnight to 0.45-μm nitrocellulose. Further details can be found in the Supplemental Appendix.

STATISTICS. Full statistical methodology can be found in the Supplemental Appendix. Briefly, all data were presented as mean ± SEM. Variables with the repeated measurements over time were analyzed using the mixed-effects model approach, and the comparisons within the treatment group between

FIGURE 3 LV Remodeling

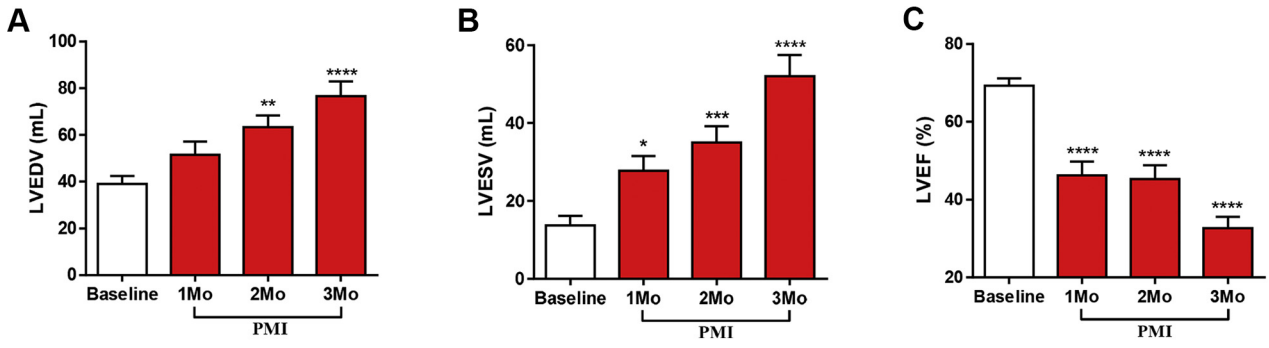

Echocardiography was performed before, 1 month (Mo), 2Mo, and 3Mo post-myocardial infarction (PMI). **(A)** Left ventricular (LV) end-diastolic volume (LVEDV), **(B)** end-systolic volume (LVESV), and **(C)** ejection fraction (LVEF) images were acquired using the 2-dimensional parasternal long-axis view. Calculation was performed using the Simpson method. **Open bars** represent before MI, **red bars** represent PMI. *p ≤ 0.05; **p ≤ 0.005; ***p ≤ 0.005; ****p ≤ 0.005 versus baseline.

different time points or between each of the post-MI time points and the baseline were made simultaneously via the Tukey-Kramer or Dunnett-Hsu adjustment. Bonferroni adjustment was employed for any other nonexhaustive multiple pairwise comparisons within the group. However, no adjustment was made for comparisons of ±DOB (i.e., before and after DOB treatment) at a given time point within the group (i.e., baseline ± DOB, 3 months ± DOB, and RBX 3 months ± DOB). Hemodynamics data were analyzed using the mixed-effects regression model in a similar fashion as described previously in the text (32). A p value <0.05 was considered statistically significant. All analyses were performed using SAS version 9.3 (SAS Institute, Cary, North Carolina).

RESULTS

VENTRICULAR REMODELING AFTER MI. IR of the LAD distribution caused a large MI. The total scar volume of IR/MI hearts was 17% of total ventricular volume (Figures 2A to 2C). Three months after MI, the infarct area was largely scar tissue and the border zone also had significant scarring (Figure 2D). MI hearts had significant increases in the heart weight/body weight ratio, documenting a reactive hypertrophic response (Figure 2E). Wheat germ agglutinin staining was used to quantify myocyte cross-sectional area in the border zone and remote zone tissue. Myocyte size was significantly increased, versus shams, in both zones (Figure 2F). Associated with the structural remodeling, we also observed alteration in the molecular activation of PKCα. A significant increase in the membrane-bound PKCα fractions was observed at 3 months post-MI. Membrane translocation of PKCα indicates increased activity (33) and is thought to be one mechanism contributing to the reduced contractility at 3 months post-MI (Figure 2G).

Temporal changes in cardiac structural and functional remodeling after MI were defined with serial echocardiogram analysis. Cardiac structural and functional remodeling after MI were also assessed with invasive hemodynamic measurements, including pressure volume determinations and DOB stress responses that were performed before and 3 months after MI (Figures 3 to 5). Progressive cardiac chamber dilation (increased LV end-diastolic volumes [LVEDVs] and LV end-systolic volumes [LVESVs]) was associated with progressive decreases in ventricular performance (LVEF) over the 3 months following MI (Figures 3A to 3C). Invasive hemodynamic measurements made before MI and then repeated during terminal studies confirmed the longitudinal echocardiographic findings (Supplemental Table 1). LV pressure and volume measurements showed that the EDPVR was shifted to larger volumes at spontaneous heart rates (Figures 4A and 4B). The LV volume at an end-diastolic pressure of 10 mm Hg (LVVPed10) was also increased, confirming dilation (Figure 4D). EF was found to be significantly reduced versus baseline (71.61 ± 4.16% to 35.55 ± 2.52%) at 3 months post-MI (Figure 4F). The rightward shift in the ESPVR (Figures 4A and 4B) and increased LVVPes80 (Figure 4E) indicate reduced ventricular contractility 3 months post-MI. The pre-load recruitable stroke work (PRSW), which is a load-independent measurement of systolic function, was significantly shifted toward the right at 3 months post-MI (Figure 4C),

FIGURE 4 Hemodynamic Deterioration due to Acute MI

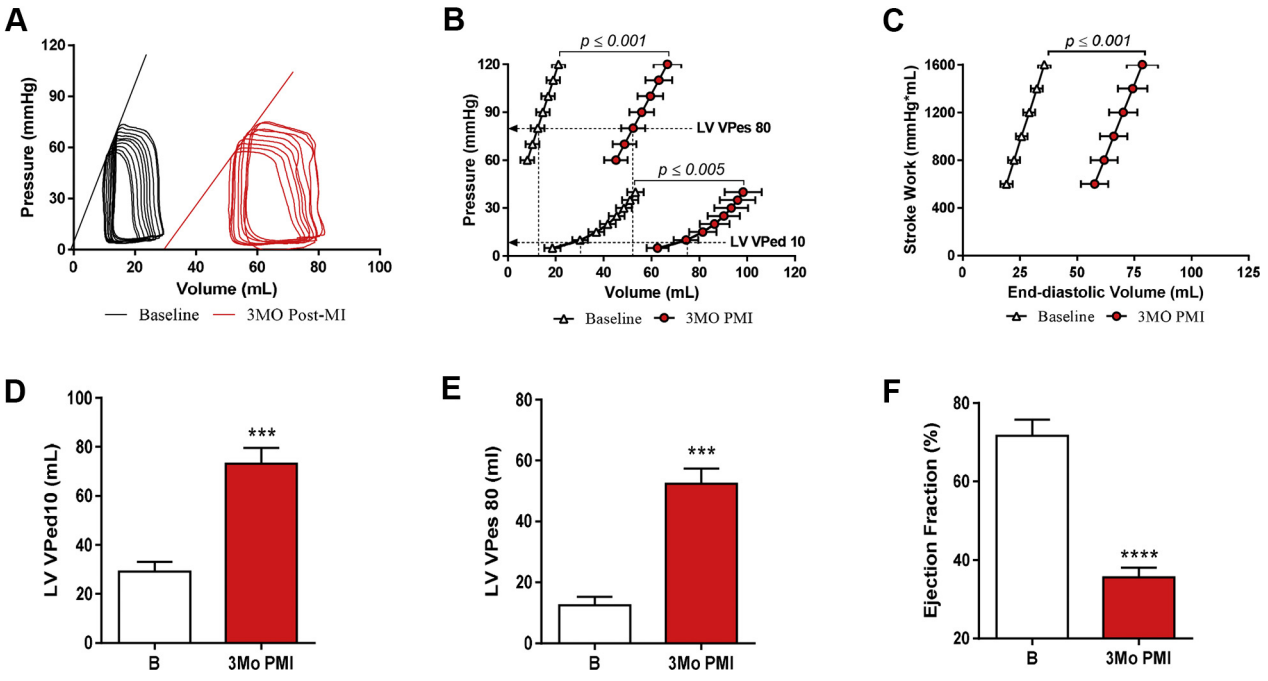

Invasive hemodynamics were performed at baseline and 3 months PMI. **(A)** Representative pressure-volume loops from before and 3 months after MI. **(B)** Both end-systolic pressure-volume relationship (ESPVR) and end-diastolic pressure volume relationship (EDPVR) are shown. ESPVR and EDPVR are shifted rightward at 3 months PMI versus baseline. **(C)** The pre-load recruitable stroke work (PRSW), a load-independent measure. is significantly reduced after MI. **(D)** LV volume at pressure of 10 mm Hg (LVVPed10) was significantly increased post MI, indicating an increase in capacitance. **(E)** LVVPes80 was also significantly increased, indicating a reduction in contractility as it pertains to the fore of contraction. **(F)** Left ventricular ejection fraction was reduced, indicating dilation at 3 months after MI. ***$p \leq 0.001$, ****$p \leq 0.0005$ versus baseline (B). Abbreviations as in Figure 2.

showing a decreased amount of work being performed for a given volume. There was also widening of the QRS complex at 3 months post-MI, suggesting electrical remodeling, likely due to scar formation and diffuse fibrosis within the remote zone (Supplemental Table 2). These functional data confirmed the development of a HFrEF phenotype in these animals at 3 months post-MI.

DOB's EFFECTS 3 MONTHS POST-MI ARE REDUCED. Cardiac inotropic responses to DOB (2.5 μg/kg/min) were measured before and 3 months after MI (**Figure 5,** Supplemental Table 1). This DOB concentration was chosen because it produced a doubling of the dP/dT max at baseline (30). DOB infusion caused significant changes in ESPVR (specifically the E_{es}), LVVPes80, and dP/dTmax in the normal heart (**Figures 5C, 5F, and 5H,** Supplemental Table 1). DOB infusions performed at baseline were repeated in the same animals 3 months after MI. At 3 months post-MI, the overall DOB effects were reduced and only caused significant changes in dP/dTmax and PRSW (Supplemental Table 1.0), whereas changes in ESPVR and $LVVP_{es}80$ were statistically insignificant. These experiments demonstrate that the effects of DOB on cardiac contractility are reduced in this IR/MI HFrEF model.

RBX REDUCES FILLING VOLUMES AND INCREASES CONTRACTILITY. Transthoracic echocardiography and invasive hemodynamics were performed after RBX administration in 3 months post-MI and control animals. The most significant effect of RBX in MI hearts was a significant reduction in the LV volumes, consequentially leading to an increased LVEF as measured by echocardiography (**Figures 6A to 6C**). Echocardiography measurements also showed that RBX had no significant effect on cardiac filling volumes or LVEF in age-matched controls (**Figures 6D to 6F**). The significant reduction in EDVs and ESVs in MI + RBX was confirmed with invasive hemodynamics (Supplemental Table 1). These studies showed a significant leftward shift in the pressure-volume loop, EDPVR, and LVVPed10 (**Figures 7A, 7B, and 7E**).

FIGURE 5 Altered Hemodynamic Response to DOB 3 Months PMI

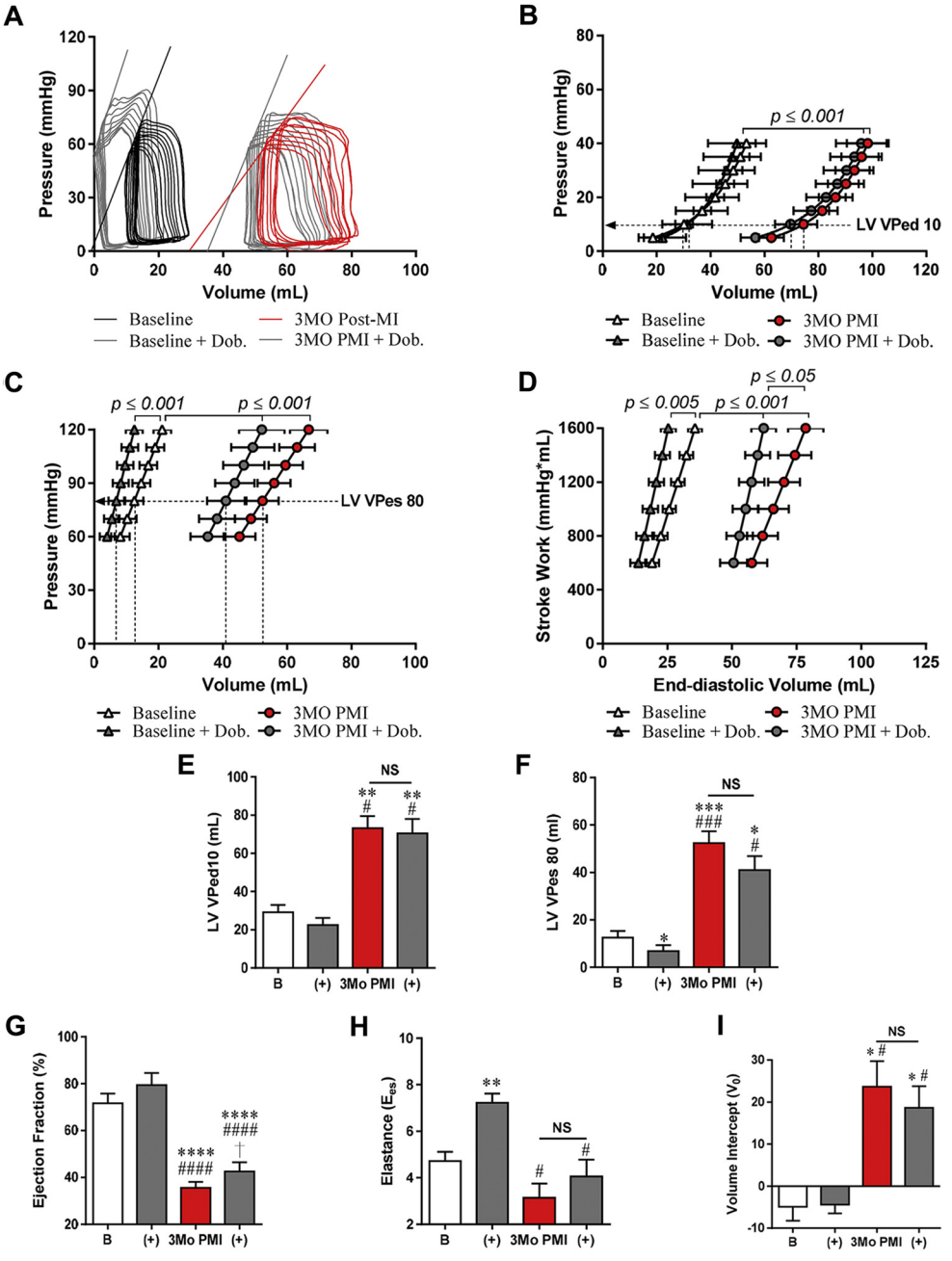

Invasive hemodynamics were performed at baseline ± DOB and 3 months PMI ± DOB. **(A)** Representative pressure-volume loops in the presence and absence of DOB at baseline and 3 months after MI. **(B)** EDPVR was not altered at either time point ± DOB. **(C)** ESPVR was significantly altered (specifically the Ees) at baseline ± DOB, but not at 3 months PMI. **(D)** PRSW was increased at both time points. **(E)** LVVPed10 was not significantly reduced in the presences of DOB at 3 months PMI. **(F)** The LVVPes80 was significantly reduced at baseline ± DOB, but not 3 months PMI ± DOB. **(G)** EF was increased significantly by DOB at 3 months PMI, but only due to modest reduction in ESV. **(H)** The Ees, 1 of 2 determinants of the ESPVR, was significantly increased at baseline + DOB, but not at 3 months PMI. **(I)** The volume intercept, second determinant of the ESPVR, was not significantly changed at 3 months PMI ± DOB. **Open bars** = baseline (B), and **gray bars** = dobutamine (+), **red bars** = 3Mo PMI. *p ≤ 0.05, **p ≤ 0.005, ***p ≤ 0.001, ****p ≤ 0.0005 versus baseline; †p ≤ 0.05 versus 3 months PMI; #p ≤ 0.05, ###p ≤ 0.001, ####p ≤ 0.0005 versus baseline + DOB. NS = nonsignificant; other abbreviations as in Figures 1, 2, and 4.

FIGURE 6 Assessment of LV Volumes With RBX Treatment After MI and in Control Animals

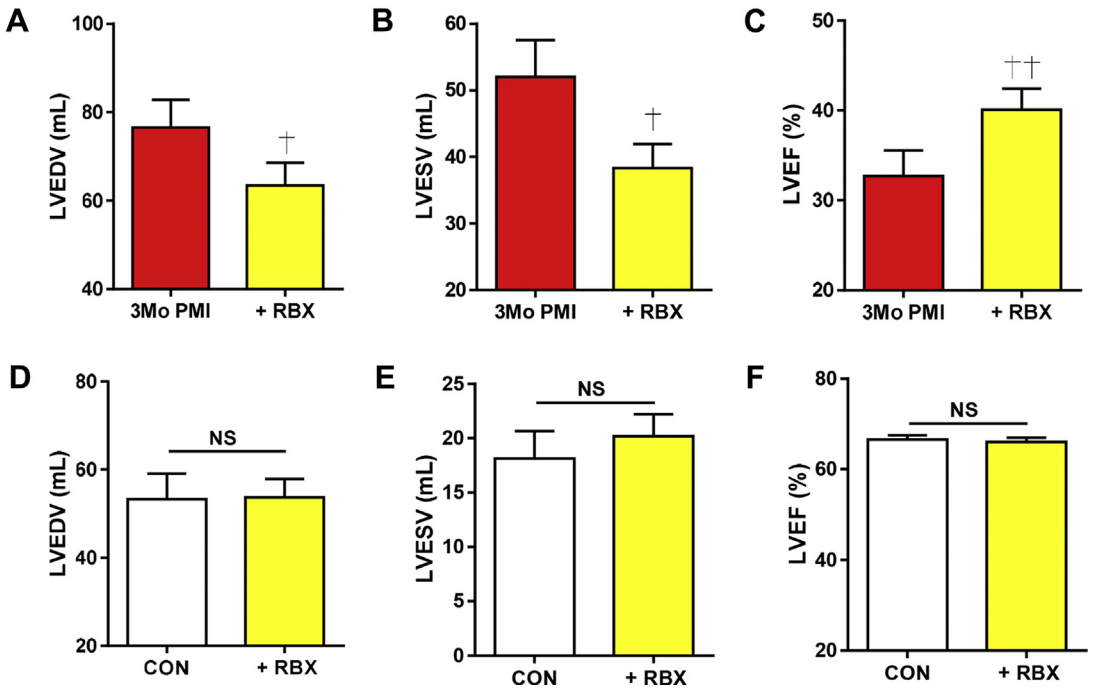

Echocardiography was performed before and after RBX treatment at 3 months PMI. **(A)** Left ventricular (LV) end-diastolic volume (LVEDV) was reduced + RBX. **(B)** LV end-systolic volume (LVESV) was reduced + RBX. **(C)** LV ejection fraction (LVEF) was increased + RBX. In age-matched controls (CON), ± RBX had no effect on **(D)** LVEDV, **(E)** LVESV, or **(F)** LVEF. Images were acquired using the 2-dimensional parasternal long-axis view. Calculation was performed using the Simpson method. †$p \leq 0.05$, ††$p \leq 0.005$ versus 3 months PMI. Abbreviations as in Figures 1, 2, and 4.

In the presence of RBX treatment, the ESPVR and the load-independent measure, PRSW, shifted significantly leftward back toward baseline, whereas the LVVPes80 was substantially reduced (Figures 7C, 7D, and 7F), demonstrating an increase in force of contraction. Although the marginal increase in E_{es} was not significant versus 3 months PMI + DOB, the V_o was significantly reduced (Figures 7H and 7I).

ECG measurements were made in RBX-treated animals. RBX increased the heart rate, but there were no other statistically significant alterations in ECG intervals (Supplemental Table 2). In control swine, RBX had no statistically significant effects on cardiac function (Figures 6D to 6F) or on rate, rhythm, or conduction (Supplemental Table 2). No arrhythmias were observed in any RBX-treated control or MI animals.

RBX ALTERS PKCα PHOSPHORYLATION WITHOUT ALTERATIONS OF KEY PKA DOWNSTREAM TARGET. Tissue samples were collected from (remote zone) explanted hearts at 3 months post-MI ± RBX to determine whether RBX caused changes in PKCα activity or phosphorylation of the PKA target protein phospholamban (PLN) (Figure 8). Many phosphorylation sites are thought to induce changes in PKCα activity, including threonine 638 (T638). In the presence of RBX, PKCα phosphorylation at T638 was decreased as compared with MI animals without treatment (Figure 8A). The reduction of PKCα T638 phosphorylation was associated with significant RBX improvements in cardiac structure (LVEDV and LVESV) and function (LVEF) (Figure 8B). PLN is a critical regulator of sarcoplasmic reticulum Ca^{2+}-ATPase (SERCA) activity and is directly phosphorylated by PKA at serine-16. We found that RBX had no statistically significant effect on PLN-S16 phosphorylation (Figure 8B).

DISCUSSION

MI, which causes death of the affected tissue, is followed by cardiac remodeling, which involves scar formation, ventricular dilation, and poor pump function. Ultimately, this remodeling can lead to HFrEF. A critical feature of this syndrome is persistent neuroendocrine responses that are required to

FIGURE 7 RBX Reduces EDPVR and Improves Contractility

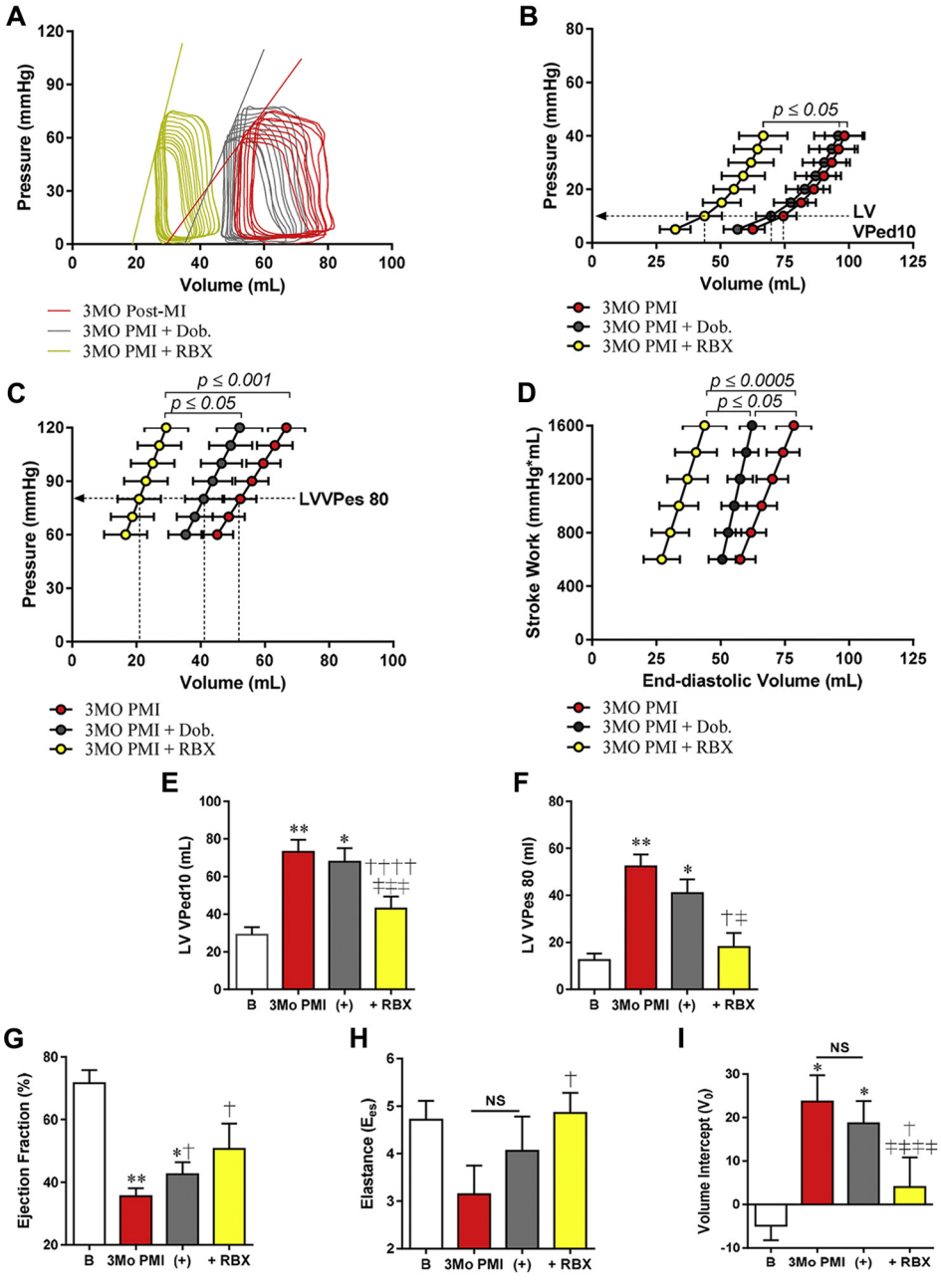

Serial invasive hemodynamics were performed at baseline (B), 3 months PMI ± DOB, and ± RBX. **(A)** Representative pressure-volume loops at 3 months after MI + DOB or + RBX. **(B)** EDPVR was not altered ± DOB, but shifted leftward with RBX. **(C)** ESPVR was not significantly altered 3 months PMI + DOB but was also shifted leftward with RBX. **(D)** PRSW was increased at both time points but to a greater extend with RBX. **(E)** LVVPed10 was significantly reduced in the presence of RBX at 3 months PMI versus 3 months PMI +DOB. **(F)** The LVVPes80 was significantly reduced at 3 months PMI +RBX, but not ± DOB. **(G)** EF was increased significantly by DOB and RBX at 3 months PMI, but due to profound reductions in the EDV with RBX. **(H)** The E_{es}, 1 of 2 determinants of the ESPVR, was significantly increased at +RBX versus 3 months PMI. **(I)** The volume intercept, second determinant of the ESPVR, was significantly changed at 3 months PMI + RBX vs. ± DOB. RBX **(yellow bars** = 2.5 μg/kg/min RBX. *p ≤ 0.05, **p ≤ 0.005 versus baseline; †p ≤ 0.05, ††††p ≤ 0.0005 versus 3 months PMI; ‡p ≤ 0.05, ‡‡‡p ≤ 0.001, ‡‡‡‡p ≤ 0.0005 versus 3 months PMI + DOB. Abbreviations as in Figures 1, 2, and 4.

FIGURE 8 RBX Reduces PKCα Phosphorylation at T638 and Does Not Directly Alter PKA-Dependent Signaling

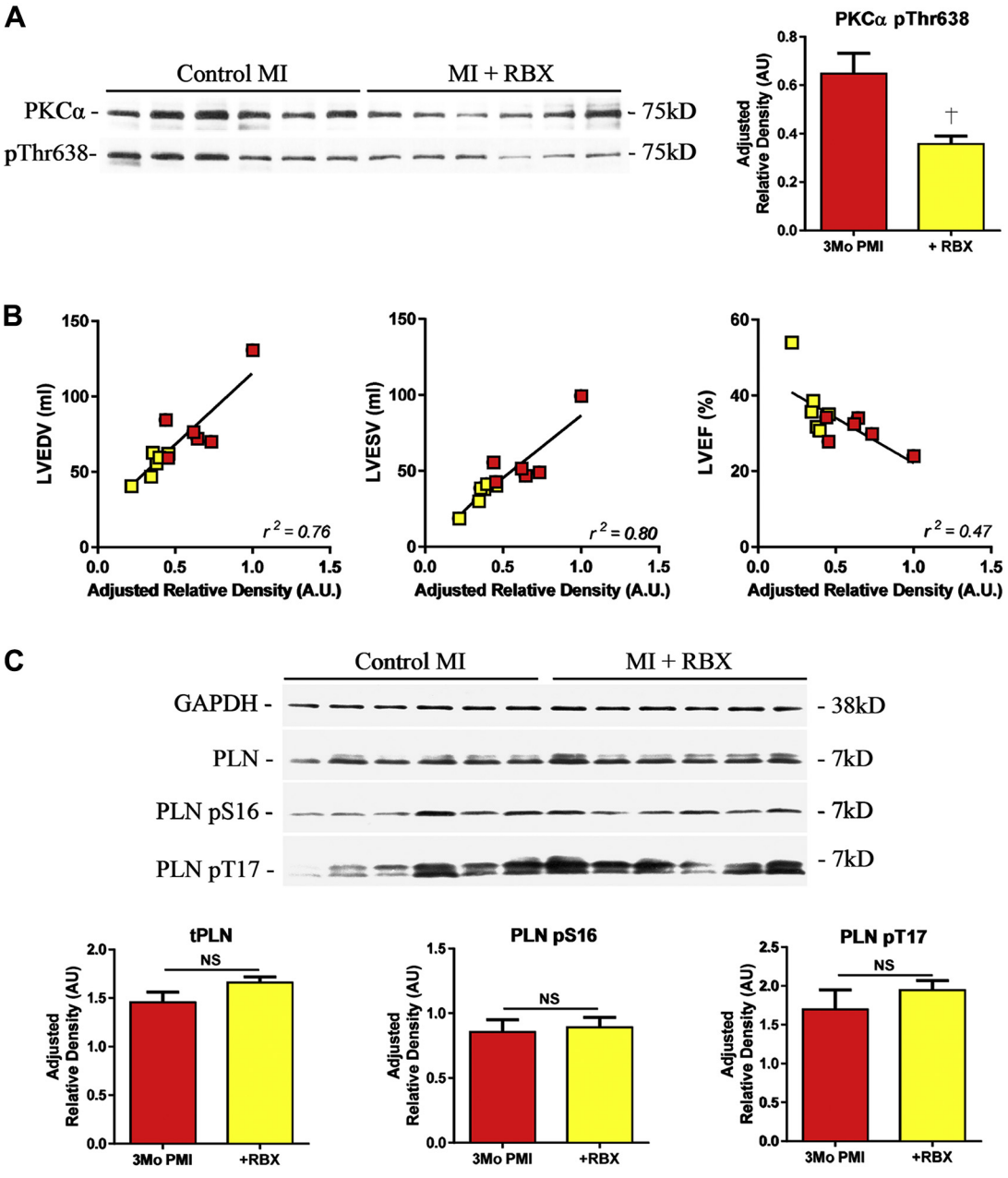

(A) Western blot for total PKCα and phosphorylation at threonine 638 (T638) after MI ± RBX. T638 phosphorylation was reduced in the presences of RBX **(B)** Correlation of T638 phosphorylation and echocardiographic volumetric analysis. Increased phosphorylation was positively correlated to increases in LVEDV and LVESV at 3 months PMI, and reduced LVEF. **(C)** Western blot for total phospholamban (PLN) and phosphorylation sites, serine 16 (S16) and threonine 17 (T17). RBX had no effect on the S16 or T17 phosphorylation. †$p \leq 0.05$ versus 3 months PMI. Abbreviations as in Figures 1, 2, 4, and 5.

maintain basal hemodynamics but eventually lead to reduced inotropic reserve (1,23). Myocyte remodeling, including reduced effects of β-adrenergic signaling on downstream inotropic target proteins, are critical components of reduced inotropic reserve in HF (34).

Activation of PKCα is known to reduce cardiac contractility in rodents (10,12). PKCα activity is

modest in the normal heart, but is increased in cardiac hypertrophy and failure, and contributes to the reduced inotropic reserve of the failing heart by altering contractile Ca^{2+} regulation (12) and properties of myofibrillar proteins (35–38). Patients with acute decompensated or severe HF often require inotropic therapies to maintain systemic blood pressure. These patients have reduced contractility reserve because those signaling cascades that increase contractility are blunted (PKA) and because those that decrease inotropy (PKCα) are enhanced. Classical (positive) inotropic agents, including cardiac glycosides and β-adrenergic agonists, have been employed to enhance contractility in HF (39). These agents increase cardiac function, but unfortunately, they can have side effects that limit their usefulness (40,41). The most significant side effect is ventricular arrhythmias that can cause sudden death (5). Other negative effects result from the induced Ca^{2+} overload, which can promote myocyte death, and this contributes to HF progression. There is a need for the development of novel inotropic therapies that can produce either short- or long-term increases in cardiac contraction without inducing arrhythmias or cell death. The rationale for PKCα antagonist therapy is that it would relieve the negative influences of PKCα activity on contractility without enhancing stimulation of the dysfunctional β-adrenergic signaling cascade.

DOB EFFECTS ON VENTRICULAR CONTRACTILITY ARE REDUCED IN THE SWINE MI MODEL. IR/MI in the swine causes profound cardiac remodeling, with scar formation, ventricular dilation, and reduction in cardiac contractility. Reduced effects of sympathetic agonists in the failing heart are well described (42) and result from persistent sympathetic input to the heart as HF develops and progresses. The molecular bases of reduced β-adrenergic responsiveness include receptor desensitization (43) and internalization, as well as changes in PKA target-protein phosphorylation. Our swine model has early features of blunted adrenergic responsiveness as evidenced by reduced DOB effects on contractility as compared with baseline β-adrenergic responses.

RBX INCREASES CARDIAC CONTRACTILITY IN A HFrEF MODEL. The effects of RBX on cardiac function were measured in normal age-matched controls and in animals 3 months after MI. RBX had no statistically significant effects on cardiac function in normal animals, suggesting that PKCα activity in the normal swine heart is low, consistent with results in rodent models and patients (33,44). In the presence of early structural and functional abnormalities observed in HF (i.e., ventricular dilation, dampened β-adrenergic responsiveness), RBX produced increases in cardiac contractility, as evidenced by a leftward shift in the ESPVR, an increase in the E_{es}, and reduced LVVPes80 in our pig model of HFrEF. RBX had no significant effects in normal animals. These results are consistent with the idea that PKCα activity increases in MI heart, and this contributes to the depressed contractility. Our results suggest that these contractility defects can be reversed with PKCα antagonism, consistent with related studies in rodents and other large animals (8–12,24).

RBX CAUSES REDUCTIONS IN FILLING VOLUMES. LVEDV increased with time after MI, as determined with both echocardiography (LVEDV) and invasive hemodynamic (V_{ed}) measurements and consistent with other models of dilated cardiomyopathy secondary to ischemia (45). DOB did not significantly reduce end-diastolic volume at 3 months post-MI, whereas RBX caused a significant reduction in LV filling volume and caused a leftward shift of the EDPVR in the same MI animals in which DOB had little effect on these parameters. The reduction in EDV and the increased contractility caused by RBX would be expected to reduce the energetic demands of the HFrEF heart.

RBX effects are similar to those caused by cardiac glycosides, such as digitalis (DIG), in HFrEF patients (46). DIG has been studied for its positive inotropic effects for over 2 centuries (47). DIG causes a reduction in heart size as evident by improved EF (48) and increased contractility via inhibition in the sodium-potassium ATPase and subsequent increase in cytosolic Ca^{2+}; and despite some limitations, it is still in clinical use (49). The bases of the RBX-induced reduction in EDV are not clear and need to be studied further. We did not observe any arrhythmogenic effects of RBX, suggesting it may be a positive inotrope without significant proarrhythmogenic characteristics. These data are corroborated with some 17 clinical trials previously performed by Eli Lilly (27,50,51), in patients who were diabetic and more likely to have underlying cardiovascular disease, but did not suffer an adverse cardiac event such as arrhythmias, although arrhythmia or sudden death was not reported in any of these trials.

RBX INHIBITS PKCα INHIBITION OF CONTRACTILITY WITHOUT PKA-MEDIATED β-ADRENERGIC AGONISM. PKCα is activated through diacylglycerol (DAG), multiple phosphorylation sites, and Ca^{2+} binding (52–54). Phosphorylation site (T638) influences PKCα's sensitivity to phosphatases, and reduced T638 phosphorylation leads to subsequent inhibition of PKCα (55). In the presence of RBX, we observed a

reduction in T638 phosphorylation, consistent with our idea that PKCα inhibition led to observed increases in contractility in MI hearts. We also determined that RBX effects were not related to changes in the phosphorylation of PLN, a nodal regulator of SERCA activity, and a direct downstream target of PKA. Therefore, RBX appears to have inotropic effects that are independent of PKA signaling cascades.

CONCLUSIONS

Our results demonstrate that RBX significantly increases cardiac function in an IR/MI model of HFrEF. RBX had no statistically significant inotropic or EDV-modifying effects in normal swine, consistent with our finding that PKCα activity is lower in the normal heart and increases with disease progression. Others have found that PKCα activity increases in proportion to disease burden (33,56). Therefore, positive inotropic effects of RBX should increase with disease severity. This stands in contrast with inotropic agents that rely on activation of PKA signaling. The disruption in PKA signaling increases with disease severity so that inotropic responsiveness to agents like DOB are reduced in proportion to disease (42,43). Our new results suggest that RBX might be an effective inotropic therapeutic agent in severe HF, when PKA signaling is significantly depressed and PKCα activity is expected to be high. These new data, along with our previous work (8–12), suggest that increased PKCα activity in HF contributes to depressed myocyte contractility and that PKCα inhibition with RBX can improve cardiac function and reduce heart size. Given RBX's safety profile (25), our results suggest a clinical trial in HF patients may be warranted.

ADDRESS FOR CORRESPONDENCE: Dr. Steven R. Houser, Temple University, Lewis Katz School of Medicine, 3500 North Broad Street, Medical Education Research Building 10th Floor, Philadelphia, Pennsylvania 19140. E-mail: SRHouser@temple.ed.

PERSPECTIVES

COMPETENCY IN MEDICAL KNOWLEGDE: HFrEF patients with acute decompensated HF can require inotropic support for hemodynamic stabilization. Most current inotropic therapeutics signal through PKA-dependent pathways (i.e., dopamine, dobutamine, and isoprenaline) or by inhibition of the phosphodiesterase that inactivates cAMP activity (i.e., milrinone). The lethal arrhythmias and exacerbation of HF symptoms in patients who have received inotropic support is a major concern in the current clinical guidelines. We have identified a potential novel target, PKCα, which is up-regulated in HF patients and negatively regulates contractility in models of HF. We have found that the PKCα inhibitor, ruboxistaurin (RBX), reduces heart size and improves cardiac pump function in a HFrEF large animal model.

TRANSLATIONAL OUTLOOK: RBX has been used in previous clinical trials for other potential applications and shown to have a solid safety profile and is well tolerated. There are several small-animal models indicating that PKCα is a negative regulator of contractility in disease, with increased activity observed in HF patients. The present study showed that RBXs reduced PKCα activity and enhanced cardiac function in a large HFrEF animal model. Our results suggest that RBX might be repurposed as a therapeutic for HFrEF.

REFERENCES

1. Braunwald E. Research advances in heart failure: a compendium. Circ Res 2013;113:633–45.

2. von Lueder TG, Krum H. New medical therapies for heart failure. Nat Rev Cardiol 2015;12:730–40.

3. Hampton JR, van Veldhuisen DJ, Kleber FX, et al., Second Prospective Randomised Study of Ibopamine on Mortality and Efficacy (PRIME II) Investigators. Randomised study of effect of ibopamine on survival in patients with advanced severe heart failure. Lancet 1997;349:971–7.

4. Lohse MJ, Engelhardt S, Eschenhagen T. What is the role of β-adrenergic signaling in heart failure? Circ Res 2003;93:896–906.

5. Thackray S, Easthaugh J, Freemantle N, Cleland JG. The effectiveness and relative effectiveness of intravenous inotropic drugs acting through the adrenergic pathway in patients with heart failure-a meta-regression analysis. Eur J Heart Fail 2002;4:515–29.

6. Fonarow GC, Abraham WT, Albert NM, et al. Factors identified as precipitating hospital admissions for heart failure and clinical outcomes: findings from OPTIMIZE-HF. Arch Intern Med 2008;168:847–54.

7. Felker GM, Leimberger JD, Califf RM, et al. Risk stratification after hospitalization for decompensated heart failure. J Card Fail 2004;10:460–6.

8. Braz JC, Bueno OF, De Windt LJ, Molkentin JD. PKCα regulates the hypertrophic growth of cardiomyocytes through extracellular signal-regulated kinase1/2 (ERK1/2). J Cell Biol 2002;156:905–19.

9. Hambleton M, York A, Sargent MA, et al. Inducible and myocyte-specific inhibition of PKCα enhances cardiac contractility and protects against infarction-induced heart failure. Am J Physiol Heart Circ Physiol 2007;293:H3768–71.

10. Liu Q, Chen X, MacDonnell SM, et al. Protein kinase cα, but not PKCβ or PKCγ, regulates contractility and heart failure susceptibility: implications for ruboxistaurin as a novel therapeutic approach. Circ Res 2009;105:194–200.

11. Hambleton M, Hahn H, Pleger ST, et al. Pharmacological- and gene therapy-based inhibition of protein kinase cα/β enhances cardiac contractility and attenuates heart failure. Circulation 2006;114:574–82.

12. Braz JC, Gregory K, Pathak A, et al. PKC-[alpha] regulates cardiac contractility and propensity toward heart failure. Nat Med 2004;10:248–54.

13. Liu Y, Lei S, Gao X, et al. PKCbeta inhibition with ruboxistaurin reduces oxidative stress and attenuates left ventricular hypertrophy and dysfunction in rats with streptozotocin-induced diabetes. Clin Sci (Lond) 2012;122:161–73.

14. Gu X, Bishop SP. Increased protein kinase C and isozyme redistribution in pressure-overload cardiac hypertrophy in the rat. Circ Res 1994;75:926–31.

15. Takeishi Y, Bhagwat A, Ball NA, Kirkpatrick DL, Periasamy M, Walsh RA. Effect of angiotensin-converting enzyme inhibition on protein kinase C and SR proteins in heart failure. Am J Physiol 1999;276:H53–62.

16. Malhotra R, D'Souza KM, Staron ML, Birukov KG, Bodi I, Akhter SA. G alpha(q)-mediated activation of GRK2 by mechanical stretch in cardiac myocytes: the role of protein kinase C. J Biol Chem 2010;285:13748–60.

17. Yang L, Doshi D, Morrow J, Katchman A, Chen X, Marx SO. Protein kinase C isoforms differentially phosphorylate Ca(v)1.2 alpha(1c). Biochemistry 2009;48:6674–83.

18. Pass JM, Gao J, Jones WK, et al. Enhanced PKC beta II translocation and PKC beta II-RACK1 interactions in PKC epsilon-induced heart failure: a role for RACK1. Am J Physiol Heart Circ Physiol 2001;281:H2500–10.

19. Ping P, Takano H, Zhang J, et al. Isoform-selective activation of protein kinase C by nitric oxide in the heart of conscious rabbits: a signaling mechanism for both nitric oxide-induced and ischemia-induced preconditioning. Circ Res 1999;84:587–604.

20. Liu Q, Molkentin JD. Protein kinase Cα as a heart failure therapeutic target. J Mol Cell Cardiol 2011;51:474–8.

21. Belin RJ, Sumandea MP, Allen EJ, et al. Augmented protein kinase C-alpha-induced myofilament protein phosphorylation contributes to myofilament dysfunction in experimental congestive heart failure. Circ Res 2007;101:195–204.

22. Dixon JA, Spinale FG. Large animal models of heart failure: a critical link in the translation of basic science to clinical practice. Circ Heart Fail 2009;2:262–71.

23. Houser SR, Margulies KB, Murphy AM, et al. Animal models of heart failure: a scientific statement from the American Heart Association. Circ Res 2012;111:131–50.

24. Ladage D, Tilemann L, Ishikawa K, et al. Inhibition of PKCα/β with ruboxistaurin antagonizes heart failure in pigs after myocardial infarction injury. Circ Res 2011;109:1396–400.

25. Aiello LP, Clermont A, Arora V, Davis MD, Sheetz MJ, Bursell SE. Inhibition of PKC beta by oral administration of ruboxistaurin is well tolerated and ameliorates diabetes-induced retinal hemodynamic abnormalities in patients. Invest Ophthalmol Vis Sci 2006;47:86–92.

26. Aiello LP, Davis MD, Girach A, et al. Effect of ruboxistaurin on visual loss in patients with diabetic retinopathy. Ophthalmology 2006;113:2221–30.

27. Aiello LP, Vignati L, Sheetz MJ, et al. Oral protein kinase c beta inhibition using ruboxistaurin: efficacy, safety, and causes of vision loss among 813 patients (1,392 eyes) with diabetic retinopathy in the Protein Kinase C beta Inhibitor-Diabetic Retinopathy Study and the Protein Kinase C beta Inhibitor-Diabetic Retinopathy Study 2. Retina 2011;31:2084–94.

28. Duran JM, Taghavi S, Berretta RM, et al. A characterization and targeting of the infarct border zone in a swine model of myocardial infarction. Clin Transl Sci 2012;5:416–21.

29. Picard MH, Adams D, Bierig SM, et al. American Society of Echocardiography recommendations for quality echocardiography laboratory operations. J Am Soc Echocardiogr 2011;24:1–10.

30. Alogna A, Manninger M, Schwarzl M, et al. Inotropic effects of experimental hyperthermia and hypothermia on left ventricular function in pigs-comparison with dobutamine. Crit Care Med 2016;44:e158–67.

31. Yeo KP, Lowe SL, Lim MT, Voelker JR, Burkey JL, Wise SD. Pharmacokinetics of ruboxistaurin are significantly altered by rifampicin-mediated CYP3A4 induction. Brit J Clinl Pharmacol 2006;61:200–10.

32. Schwarzl M, Hamdani N, Seiler S, et al. A porcine model of hypertensive cardiomyopathy: implications for heart failure with preserved ejection fraction. Am J Physiol Heart Circ Physiol 2015;309:H1407–18.

33. Bowling N, Walsh RA, Song G, et al. Increased protein kinase C activity and expression of Ca2+-sensitive isoforms in the failing human heart. Circulation 1999;99:384–91.

34. Lymperopoulos A, Rengo G, Koch WJ. Adrenergic nervous system in heart failure: pathophysiology and therapy. Circ Res 2013;113:739–53.

35. Sumandea MP, Rybin VO, Hinken AC, et al. Tyrosine phosphorylation modifies protein kinase C delta-dependent phosphorylation of cardiac troponin I. J Biol Chem 2008;283:22680–9.

36. Sumandea MP, Pyle WG, Kobayashi T, de Tombe PP, Solaro RJ. Identification of a functionally critical protein kinase C phosphorylation residue of cardiac troponin T. J Biol Chem 2003;278:35135–44.

37. Kooij V, Boontje N, Zaremba R, et al. Protein kinase C alpha and epsilon phosphorylation of troponin and myosin binding protein C reduce Ca2+ sensitivity in human myocardium. Basic Res Cardiol 2010;105:289–300.

38. Hidalgo C, Hudson B, Bogomolovas J, et al. PKC phosphorylation of titin's PEVK element: a novel and conserved pathway for modulating myocardial stiffness. Circ Res 2009;105:631–8.

39. Hasenfuss G, Teerlink JR. Cardiac inotropes: current agents and future directions. Eur Heart J 2011;32:1838–45.

40. Abraham WT, Adams KF, Fonarow GC, et al. In-hospital mortality in patients with acute decompensated heart failure requiring intravenous vasoactive medications: an analysis from the Acute Decompensated Heart Failure National Registry (ADHERE). J Am Coll Cardiol 2005;46:57–64.

41. Burger AJ, Elkayam U, Neibaur MT, et al. Comparison of the occurrence of ventricular arrhythmias in patients with acutely decompensated congestive heart failure receiving dobutamine versus nesiritide therapy. Am J Cardiol 2001;88:35–9.

42. Fowler MB, Laser JA, Hopkins GL, Minobe W, Bristow MR. Assessment of the beta-adrenergic receptor pathway in the intact failing human heart: progressive receptor down-regulation and subsensitivity to agonist response. Circulation 1986;74:1290–302.

43. Heilbrunn SM, Shah P, Bristow MR, Valantine HA, Ginsburg R, Fowler MB. Increased beta-receptor density and improved hemodynamic response to catecholamine stimulation during long-term metoprolol therapy in heart failure from dilated cardiomyopathy. Circulation 1989;79:483–90.

44. Goldberg M, Steinberg SF. Tissue-specific developmental regulation of protein kinase C isoforms. Biochem Pharmacol 1996;51:1089–93.

45. Kulandavelu S, Karantalis V, Fritsch J, et al. Pim1 kinase overexpression enhances ckit+ cardiac stem cell cardiac repair following myocardial infarction in swine. J Am Coll Cardiol 2016;68:2454–64.

46. Marchionni N, Vannucci A, Pini R, et al. Hemodynamic effects of digoxin in acute myocardial infarction. Eur Heart J 1980;1:319–26.

47. Withering W. An Account of the Foxglove, and Some of Its Medical Uses: With Practical Remarks on Dropsy, and Other Diseases. Birmingham: Printed by M. Swinney for G.G.J. and J. Robinson. London, UK: 1785.

48. Braunwald E. Effects of digitalis on the normal and the failing heart. J Am Coll Cardiol 1985;5:51A–9A.

49. Rathore SS, Curtis JP, Wang Y, Bristow MR, Krumholz HM. Association of serum digoxin concentration and outcomes in patients with heart failure. JAMA 2003;289:871–8.

50. Casellini CM, Barlow PM, Rice AL, et al. A 6-month, randomized, double-masked, placebo-controlled study evaluating the effects of the protein kinase C-beta inhibitor ruboxistaurin on skin microvascular blood flow and other measures of diabetic peripheral neuropathy. Diabetes Care 2007;30:896–902.

51. Sheetz MJ, Aiello LP, Davis MD, et al. The effect of the oral PKC beta inhibitor ruboxistaurin on vision loss in two phase 3 studies. Invest Ophthalmol Vis Sci 2013;54:1750–7.

52. Dutil EM, Newton AC. Dual role of pseudosubstrate in the coordinated regulation of protein kinase C by phosphorylation and diacylglycerol. J Biol Chem 2000;275:10697–701.

53. Bornancin F, Parker PJ. Phosphorylation of protein kinase C-alpha on serine 657 controls the accumulation of active enzyme and contributes to its phosphatase-resistant state. J Biol Chem 1997; 272:3544–9.

54. Hansra G, Garcia-Paramio P, Prevostel C, Whelan RD, Bornancin F, Parker PJ. Multisite dephosphorylation and desensitization of conventional protein kinase C isotypes. Biochem J 1999;342 Pt 2:337–44.

55. Bornancin F, Parker PJ. Phosphorylation of threonine 638 critically controls the dephosphorylation and inactivation of protein kinase Calpha. Curr Biol 1996;6:1114–23.

56. Simonis G, Briem S, Schoen S, Bock M, Marquetant R, Strasser R. Protein kinase C in the human heart: differential regulation of the isoforms in aortic stenosis or dilated cardiomyopathy. Mol Cell Biochem 2007;305: 103–11.

KEY WORDS acute myocardial infarction, heart failure with reduced ejection fraction, invasive hemodynamics, PKCα/β inhibitor, positive inotropy

APPENDIX For an expanded Methods section and supplemental figure and tables, please see the online version of this paper.